ISBN: 978-3-95450-168-7 doi:10.18429/JACoW-IPAC2015-MOPJE058

FLUKA MODELING OF THE ESS ACCELERATOR

L. Lari, L.S. Esposito, ESS, Lund, Sweden and CERN, Geneva, Switzerland
M. Eshraqi, L. Tchelidze, ESS, Lund, Sweden
F. Cerutti, A. Mereghetti, CERN, Geneva, Switzerland

Abstract

In order to evaluate the energy deposition and radiation issues concerning the ESS accelerator, a FLUKA model of the machine has been created. The geometry of the superconducting beam line is built according to the machine optics, described in the TraceWin file and the CATIA drawings of the beam elements, using the LineBuilder tool developed at CERN. The objective is to create a flexible FLUKA model that is able to be adapted to the optimization of the optics, design modifications and machine integration constraints. Preliminary results are also presented.

INTRODUCTION

The European Spallation Source (ESS) is a high-energy and a high-intensity accelerator-driven facility, currently under construction at Lund, in Sweden [1]. The ESS superconducting linac is designed to accelerate protons up to 2 GeV (kinetic energy) and to provide an average beam power of 5 MW on target. Table 1 summarizes the main accelerator parameters, while the general layout of the ESS linear accelerator is shown in Fig. 1.

Table 1: Key Parameters of the ESS Proton Linac

Average Beam Power	5 MW
Peak Beam Power	125 MW
Beam on target	> 95% availability
Proton kinetic energy	2 GeV
Pulse frequency	2.86 ms
Pulse frequency	14 Hz
Peak current	62.5 mA

The proton beam from the Ion Source is transported through a Low Energy Beam Transport (LEBT) section to the Radio Frequency Quadrupole (RFQ) for bunching and acceleration. At the extraction of the RFQ, the beam is transported and matched to the normal conducting Drift Tube Linac (DTL) through a Medium Energy Beam Transport (MEBT) section. Downstream of the 5 DTL tanks, the beam enters the superconducting part of the linac, where it is accelerated via superconducting radio frequency cavities, constructed from niobium and immersed in liquid helium at a nominal temperature of 2K. The first superconducting section contains 13 cryomodules each containing a pair of double spoke cavities. The spoke section is followed by two sections of elliptical cavities, medium-β and high-β, where β is the ratio of the proton speed to the speed of the light. In this section, the cryomodules contains 4 elliptical cavities each, for a total of 9 cryomodules for the medium-β and 21 for the high-β respectively. Finally, after acceleration, the beam is transported via the High Energy Beam Transport (HEBT) to the target.

METHODOLOGY

The effect of prompt radiation and induced radioactivity are planned to be studied with Monte-Carlo simulations. For the low energy part of the ESS linac including the DTLs included, the MCNPX code is used [2], while in the more energetic part of the accelerator (at energies outside of the neutron resonance regions), the calculations are performed with MARS [3,4] and/or FLUKA codes [5,6].

In particular, FLUKA is used to address all questions for which a detailed accelerator geometry is needed, such as activation of beam line elements and it will be used to benchmark some MARS shielding results. For this reason, a detailed FLUKA model of the ESS accelerator is in progress, starting from the last DTLs until the target and including tunnel and gallery buildings as well as stubs between tunnel and gallery, and tunnel emergency exits (see Fig. 2 for a representation of the model).

The FLUKA model of the beam line follows automatically the lattice sequence described in the official TraceWin optics output file, thanks to the LineBuilder [7]. In case of future possible hardware, footprint or optics changes, the coupling between TraceWin and LineBuilder makes possible to generate a new model, if the geometry of each element is available in FLUKA.

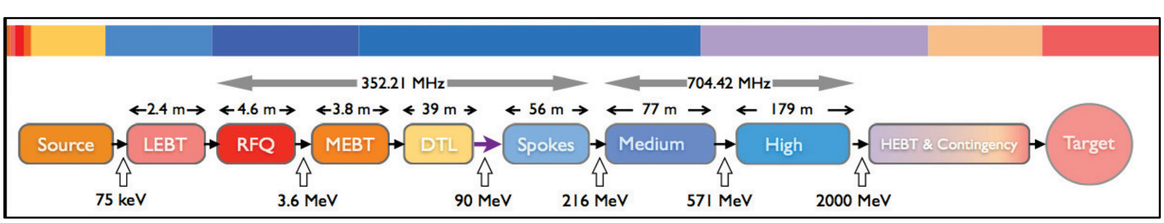

Figure 1: Schematic block diagram of the ESS accelerator lattice (bottom) and corresponding proportional length of the different sections (top). The blue items are superconducting (i.e. the spoke resonators, the medium and high β elliptical cavities), while the other items are normal conducting.

ISBN: 978-3-95450-168-7 doi:10.18429/JACoW-IPAC2015-MOPJE058

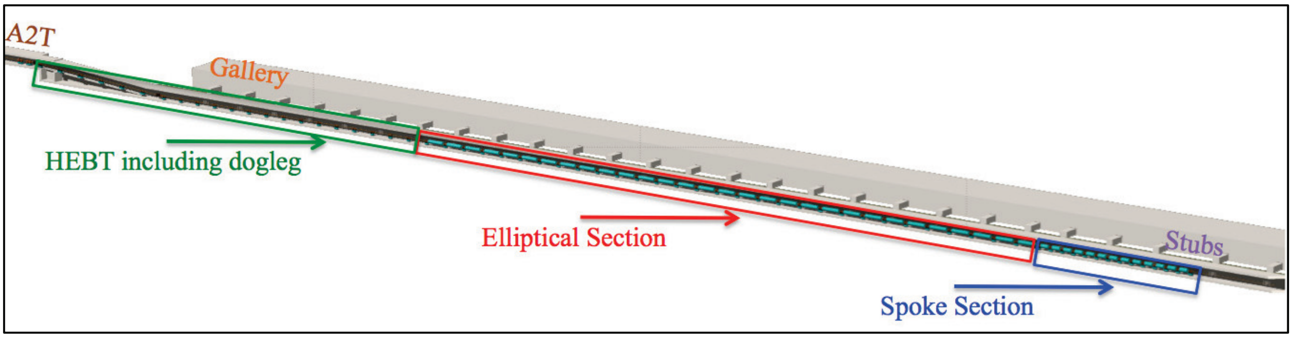

Figure 2: Current FLUKA model of the ~600 m long ESS linac. The picture shows a cut of the ESS tunnel, including the dogleg and the so-called *Accelerator to Target* (A2T) area, starting after the last dipole (i.e. at the end of the HEBT section). The elements shown are spokes and elliptical cryomodules, as well as the normal conducting magnets that focus the proton beam until the target. Two different cross-sections of the vacuum beam-pipe are used to allow a bigger aperture-to-beam size ratio as beam energy increases i.e. an internal diameter of 58.3 mm in the spoke and of 100 mm from the elliptical sections are implemented.

FLUKA routine and geometry files, together with CATIA drawings used to generate each FLUKA element are stored in a SVN repository, with the purpose of tracking any change and as historical reference for each model.

The complex FLUKA structure allows studies of realistic punctual beam losses, as well as of uniform losses distribution along the accelerator beam-pipe. In this paper, a uniform 1 W/m proton loss is considered as source term, since this value is the upper limit set by design to allow hand-on maintenance. As a conservative approach the emission angle is set to 3 mrad with respect the to the beam direction [8,9].

PRELIMINARY RESULTS

Normal conducting magnets and correctors are foreseen in the ESS accelerator to drive the beam from the proton source to the target. In particular warm quadrupoles doublets (12 in the spoke section, 30 in the elliptical section) are needed between two consecutive cryomodules, in addition to those in the HEBT (including the dogleg), and A2T area. Each doublet, housing steering magnets, is integrated in the so-called Linac Warm Unit (LWU) magnet assembly, which will also include beam diagnostics and vacuum equipment. Using pulsed power magnets to replace the water-cooled DC ones has been investigated recently. This is to remove the need for water-cooling and hence the water and manifolds from the tunnel.

The following results refer to a preliminary evaluation in terms of prompt radiation. The area covered in this study starts from the spoke section and reach the A2T region, in the range of beam energy from 90 MeV to 2 GeV. Results are normalized with respect to the total length of the beam line simulated (530 m) and the corresponding average beam energy (~633 MeV).

For the same optics [10], two magnet models have been implemented for both water-cooled DC version and pulsed power one with total and yoke lengths as reported in Table 2. QC5 magnets are located between two consecutive spokes cryomodules and QC6 ones between two elliptical cryomodules and in the HEBT area (see Fig. 3).

Table 2: QC5 and QC6 Data used in the Simulations.

	Water cooled	Pulsed
QC5 yoke length	110 mm	180 mm
QC5 total length	260 mm	280 mm
QC6 yoke length	196 mm	240 mm
QC6 total length	395.4 mm	340 mm

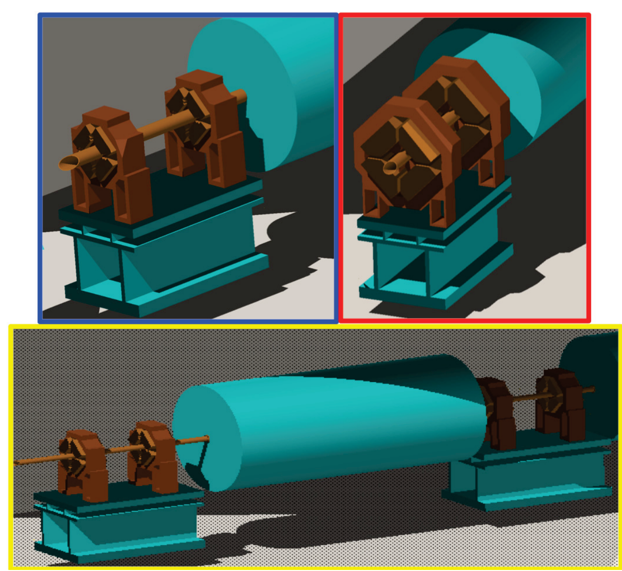

Figure 3: FLUKA model of QC6 pulsed (top left) and water cooled DC (top right) doublet magnets on their support and in front of the same elliptical cryomodule. The pulsed magnets are smaller with respect to the DC ones and they are cooled passively by air. In the bottom frame the lattice layout of QC5 pulsed magnets between spoke cryomodules is shown as example.

ISBN: 978-3-95450-168-7 doi:10.18429/JACoW-IPAC2015-MOPJE058

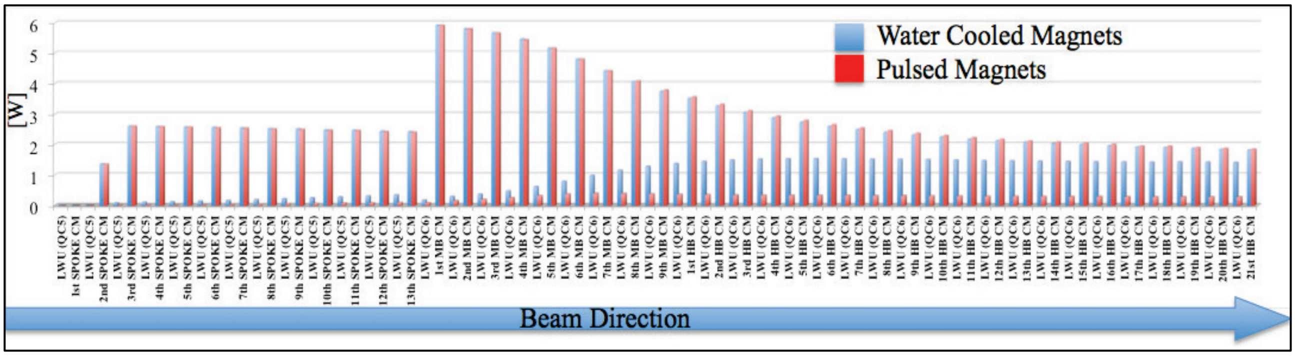

Figure 4: Integrated power on beam elements from the first spoke until the last high-β cryomodules. For the LWUs the shown values are the sum of the power in the two magnets (i.e. yokes plus coils), excluding the beam-pipe and the LWU support. Errors are less than 1%. FLUKA results about the cryomodules are of the same order of those found with MARS ones [11].

In the two cases, little variations are visible in the total power on cryomodules, while at the end of the medium-β and in the high-β section the use of the pulsed magnets is preferable to the DC ones (see Fig. 4).

Outside the beam elements, the fluence of neutrons produced in the tunnel is quite uniform (see Fig. 5). The ratio between the two designs is shown in Fig. 6.

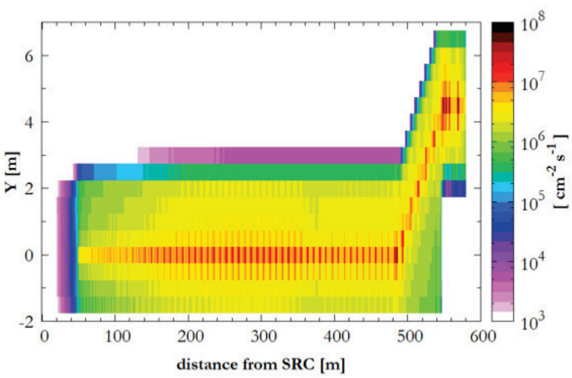

Figure 5: Neutron fluence in the tunnel from the source (SRC) and including the HEBT and A2T areas (side view). This plot refers to the water-cooled magnets.

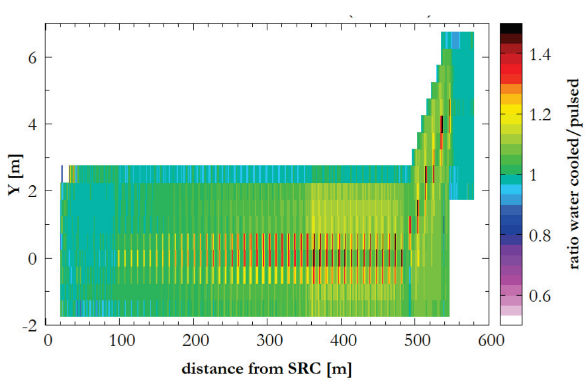

Figure 6: Neutron fluence ratio between water-cooled and air-cooled pulsed magnets. The difference is in average of the order of 10% at 1 m from the beampipe. In the HEBT area the difference is larger due to the highest impact on changing the LWU designs (see Fig. 4).

Finally the effect of the two different designs is evaluated on the last quadrupole in the A2T area (downstream dogleg dipoles), the so-called Q8 (see Fig. 7). The Q8 quadrupoles are water-cooled DC magnets and they will never been substituted by pulsed ones.

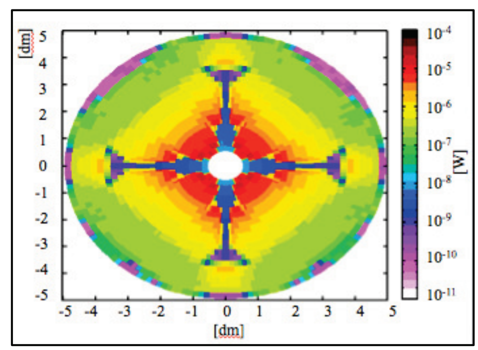

Figure 7: Integrated power deposition map on the last Q8 magnets in the A2T area in the case of pulsed magnets (in the upstream areas). A similar result is found for the water-cooled ones. As a consequence, choosing the water-cooled or pulsed magnets has no effect on the power deposited on Q8.

CONCLUSION

A detailed FLUKA model of the ESS accelerator is in progress, with the purpose of supporting the integration of the machine, benchmarking MARS or MCNPX results and performing studies on specific and/or critical topics.

In this paper, the effect of substituting the water-cooled magnets with pulsed ones, in the spokes, elliptical and HEBT section, was studied in terms of prompt radiation, using a conservative approach based on maximum allowable losses during regular operation. Apart from the power deposited on the magnets itself, no major differences were found in using the two designs. The next step is to evaluate the magnet activation during the whole lifetime of the ESS accelerator (i.e. indicative 40 years) and between the annual technical stops. Calculations on dose to the coil insulator will be also a subject of future studies to evaluate the lifetime of the magnets themselves with continuous and realistic proton losses.

ISBN: 978-3-95450-168-7 doi:10.18429/JACoW-IPAC2015-MOPJE058

REFERENCES

[1] ESS Technical Design Report, ESS 2013-001, Lund, Sweden:http://europeanspallationsource.se/scientific-technical-documentation/

[2] R. Bevilacqua et al., *Shielding calculations with MCNPX at the European Spallation Source*, Proc. SATIF-12, 28-30 April 2014, Fermilab, USA.

[3] N.V. Mokhov, *The MARS Code Sysetm User's Guide*, Fermilab-FN-628, 1995.

[4] N.V. Mokhov, S.I. Striganov, AIP Conf. Proc. 896, pp. 50-60, 2007.

[5] A. Ferrari, P.R. Sala, A. Fasso`, J. Ranft, *FLUKA: a multi-particle transport code*, CERN 2005-10 (2005), INFN/TC_05/11, SLAC-R-773.

[6] G. Battistoni, S. Muraro, P.R. Sala, F. Cerutti, A. Ferrari, S. Roesler, A. Fasso`, J. Ranft, *The FLUKA code: description and benchmarking*, Proc. Hadronic Shower Simulation Workshop 2006, 6-8 Sept 2006, Fermilab, USA.

[7] A. Mereghetti et al., *The Fluka Linebuilder and Element Database: Tools for Building Complex Models of Accelerators Beam Lines*, Proc. IPAC12, New Orleans, USA.

[8] L. Tchelidze, *Beam spill limits during various event classes (for the ESS accelerator)*, Lund, 2014.

[9] T. Hansson, *ESS Radiation Protection Strategy for Employees*, Lund, 2013.

[10] Y. Levinsen, *European Spallation Source Lattice Design Status*, presented at the 6th International Particle Accelerator Conf.(IPAC'15), Richmond, VA, USA paper THPF092, these proceedings

[11] M. Jarosz et al., *Studies into Beam Loss Patterns at European Spallation Source,* Proc. IPAC14, Dresden, Germany.